

## 8 Poincaré sections

The dynamical systems we study are of the form

$$\frac{d}{dt}\vec{x}(t) = F(\vec{x}, t)$$

Systems of such equations describe a *flow* in phase space.

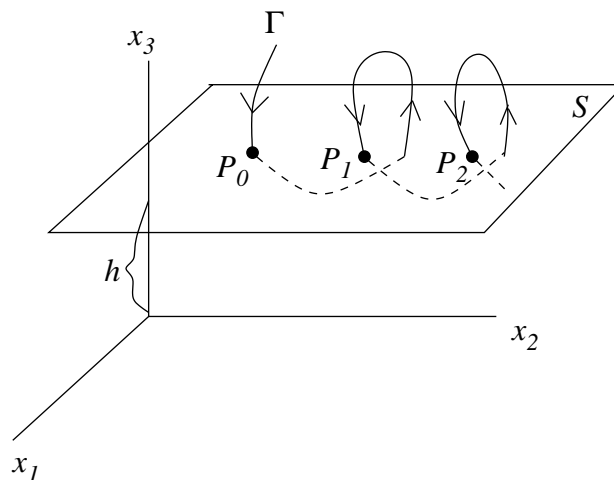
The solution is often studied by considering the trajectories of such flows.

But the phase trajectory is itself often difficult to determine, if for no other reason than that the dimensionality of the phase space is too large.

Thus we seek a geometric depiction of the trajectories in a lower-dimensional space—in essence, a view of phase space without *all* the detail.

### 8.1 Construction of Poincaré sections

Suppose we have a 3-D flow  $\Gamma$ . Instead of directly studying the flow in 3-D, consider, e.g., its intersection with a plane ( $x_3 = h$ ):



- Points of intersection correspond (*in this case*) to  $\dot{x}_3 < 0$  on  $\Gamma$ .
- Height  $h$  of plane  $S$  is chosen so that  $\Gamma$  continually crosses  $S$ .
- The points  $P_0, P_1, P_2$  form the 2-D **Poincaré section**.

The Poincaré section is a continuous mapping  $T$  of the plane  $S$  into itself:

$$P_{k+1} = T(P_k) = T [T(P_{k-1})] = T^2(P_{k-1}) = \dots$$

Since the flow is deterministic,  $P_0$  determines  $P_1$ ,  $P_1$  determines  $P_2$ , etc.

The Poincaré section reduces a *continuous* flow to a **discrete-time mapping**. However the time interval from point to point is not necessarily constant.

We expect some geometric properties of the flow and the Poincaré section to be the same:

- Dissipation  $\Rightarrow$  areas in the Poincaré section *should* contract.
- If the flow has an attractor, we should see it in the Poincaré section.

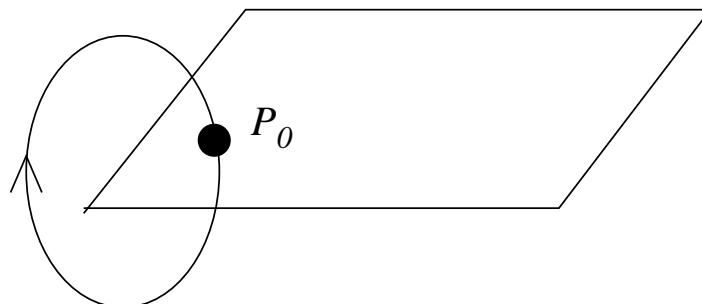
Essentially the Poincaré section provides a means to visualize an otherwise messy, possibly aperiodic, attractor.

## 8.2 Types of Poincaré sections

As we did with power spectra, we classify three types of flows: periodic, quasiperiodic, and aperiodic.

### 8.2.1 Periodic

The flow is a closed orbit (e.g., a limit cycle):



$P_0$  is a fixed point of the Poincaré map:

$$P_0 = T(P_0) = T^2(P_0) = \dots$$

We proceed to analyze the stability of the fixed point.

To first order, a Poincaré map  $T$  can be described by a matrix  $M$  defined in the neighborhood of  $P_0$ :

$$M_{ij} = \left. \frac{\partial T_i}{\partial x_j} \right|_{P_0}.$$

In this context,  $M$  is called a *Floquet matrix*. It describes how a point  $P_0 + \delta$  moves after one intersection of the Poincaré map.

A Taylor expansion about the fixed point yields:

$$T_i(P_0 + \delta) \simeq T_i(P_0) + \left. \frac{\partial T_i}{\partial x_1} \right|_{P_0} \cdot \delta_1 + \left. \frac{\partial T_i}{\partial x_2} \right|_{P_0} \cdot \delta_2, \quad i = 1, 2$$

Since  $T(P_0) = P_0$ ,

$$T(P_0 + \delta) \simeq P_0 + M\delta$$

Therefore

$$\begin{aligned} T\left(T(P_0 + \delta)\right) &\simeq T(P_0 + M\delta) \\ &\simeq T(P_0) + M^2\delta \\ &\simeq P_0 + M^2\delta \end{aligned}$$

After  $m$  iterations of the map,

$$T^m(P_0 + \delta) - P_0 \simeq M^m\delta.$$

Stability therefore depends on the properties of  $M$ .

Assume that  $\delta$  is an eigenvector of  $M$ . (There will always be a projection onto an eigenvector.) Then

$$M^m\delta = \lambda^m\delta,$$

where  $\lambda$  is the corresponding eigenvalue.

Therefore

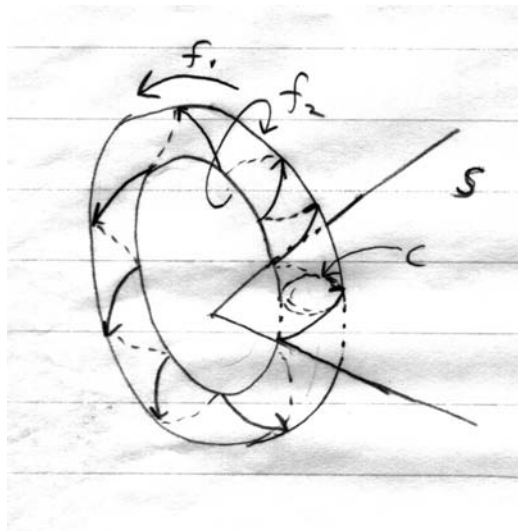
$|\lambda| < 1 \Rightarrow$  linearly stable

$|\lambda| > 1 \Rightarrow$  linearly unstable

**Conclusion:** a periodic map is unstable if one of the eigenvalues of the Floquet matrix crosses the unit circle in the complex plane.

### 8.2.2 Quasiperiodic flows

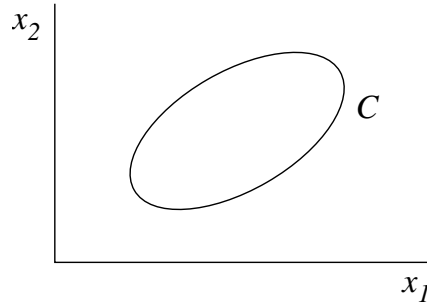
Consider a 3-D flow with two fundamental frequencies  $f_1$  and  $f_2$ . The flow is a torus  $T^2$ :



The points of intersection of the flow with the plane  $S$  appear on a closed curve  $C$ .

As with power spectra, the form of the resulting Poincaré section depends on the ratio  $f_1/f_2$ :

- **Irrational**  $f_1/f_2$ . The frequencies are called *incommensurate*. The closed curve  $C$  appears continuous, e.g.



- The trajectory on the torus  $T^2$  never repeats itself exactly.
- The curve is not traversed continuously, but rather

$$T(C) = \text{finite shift along } C.$$

• **Rational**  $f_1/f_2$ .

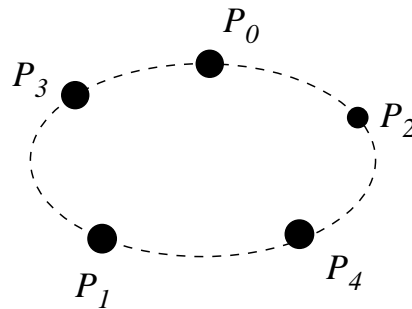
- $f_1$  and  $f_2$  are *frequency locked*.
- There are finite number of intersections (points) along the curve  $C$ .
- Trajectory repeats itself after  $n_1$  revolutions and  $n_2$  rotations.
- The Poincaré section is periodic with

$$\text{period} = n_1/f_1 = n_2/f_2$$

- The Poincaré section contains just  $n_1$  points. Thus

$$P_i = T^{n_1}(P_i)$$

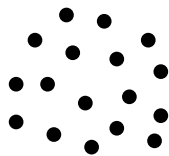
- Example,  $n_1 = 5$ :



### 8.2.3 Aperiodic flows

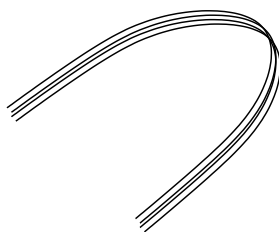
Aperiodic flows may no longer lie on some reasonably simple curve.

In an extreme case, one has just a point cloud:



This would be expected for statistical white noise.

Deterministic aperiodic systems often display more order, however. In some cases they create mild departures from a simple curve, e.g.



Such cases arise from strong dissipation (and the resulting contraction of areas in phase space).

It then becomes useful to define a coordinate  $x$  that falls roughly along this curve, and to study the iterates of  $x$ . This is called a *first return map*.

### 8.3 First-return maps

First return maps are 1-D reductions of the kind of 2-D Poincaré maps that we have been considering.

Such maps are of the form

$$x_{k+1} = f(x_k).$$

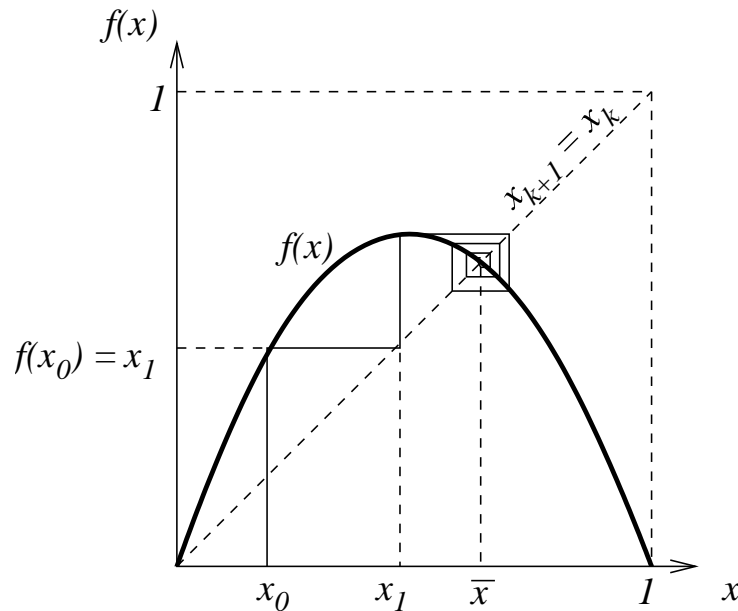
We will study these extensively at the end of the course.

We shall give particular attention to the following quadratic mapping of the unit interval onto itself:

$$x_{k+1} = 4\mu x_k(1 - x_k), \quad 0 \leq \mu \leq 1.$$

The mapping is easily described graphically. The quadratic rises from  $x = 0$ , falls to  $x = 1$ , and has its maximum at  $x = 1/2$ , where it rises to height  $\mu$ .

Consider, for example, the case  $\mu = 0.7$ :



Eventually the iterations converge to  $x = \bar{x}$ , which is where the diagonal (the identity map  $x_{k+1} = x_k$ ) intersects  $f(x)$ .

Thus  $\bar{x}$  is a fixed point of  $f$ , i.e.,

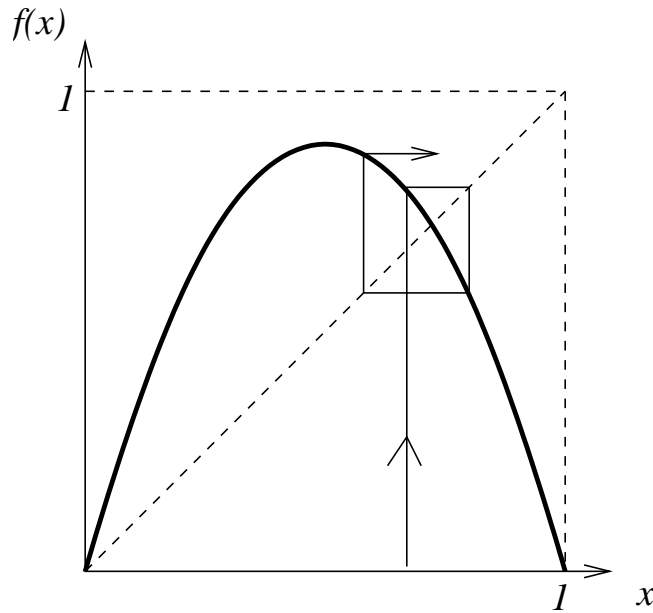
$$\bar{x} = f(\bar{x})$$

Another fixed point is  $x = 0$ , since  $f(0) = 0$ .

However we can see graphically that  $x = 0$  is unstable; iterates initiated at  $x_0 = \varepsilon$  still converges to  $\bar{x}$ .

Thus  $x = 0$  is an *unstable* fixed point, while  $x = \bar{x}$  is *stable*.

What determines stability? Consider graphically the case  $\mu = 0.9$ :



We infer that the slope  $f'(\bar{x})$  determines whether  $\bar{x}$  is stable. We proceed to show this formally.

Suppose  $x^*$  is *any* fixed point such that

$$x^* = f(x^*).$$

Define

$$x_k = x^* + \varepsilon_k, \quad \varepsilon_k \text{ small.}$$

In general, our mappings are described by

$$x_{k+1} = f(x_k).$$

Then

$$\begin{aligned} x^* + \varepsilon_{k+1} &= f(x^* + \varepsilon_k) \\ &= f(x^*) + f'(x^*)\varepsilon_k + O(\varepsilon_k^2) \end{aligned}$$

Therefore

$$\varepsilon_{k+1} \simeq f'(x^*)\varepsilon_k.$$

Thus

$$|f'(x^*)| < 1 \Rightarrow \text{stability.}$$

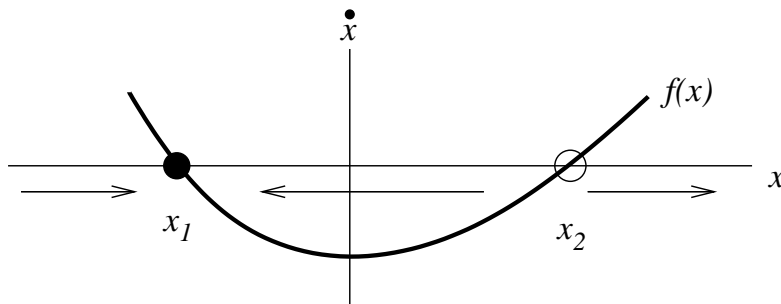


## 8.4 1-D flows

It is instructive to compare the stability of 1-D maps to the stability of the continuous 1-D flow

$$\dot{x} = f(x).$$

Consider, for example, a particular  $f(x)$  that looks like



Clearly  $x_1$  and  $x_2$  are fixed points. Which are stable?

The arrows show the direction of flow on the  $x$ -axis, i.e., the sign of  $\dot{x} = f(x)$ .

Thus  $x_1$  is stable while  $x_2$  is not.

Stability of a fixed point  $x^*$  is therefore determined as follows:

$$f'(x^*) < 0 \Rightarrow \text{stable}$$

$$f'(x^*) > 0 \Rightarrow \text{unstable}$$

Whereas the stability of a continuous 1-D flow  $f$  depends on the sign of  $f'$ , the stability of a 1-D map depends on the magnitude  $|f'|$ .

In higher dimensions this same distinction holds for the eigenvalues  $\lambda$  of the Jacobian (which, in the case of mappings, we have called the Floquet matrix). That is, the sign of  $\text{Re}(\lambda)$  determines the stability of flows, whereas the magnitude  $|\lambda|$  is the relevant quantity for maps.

## 8.5 Relation of flows to maps

We now consider explicitly how flows may be related to maps.

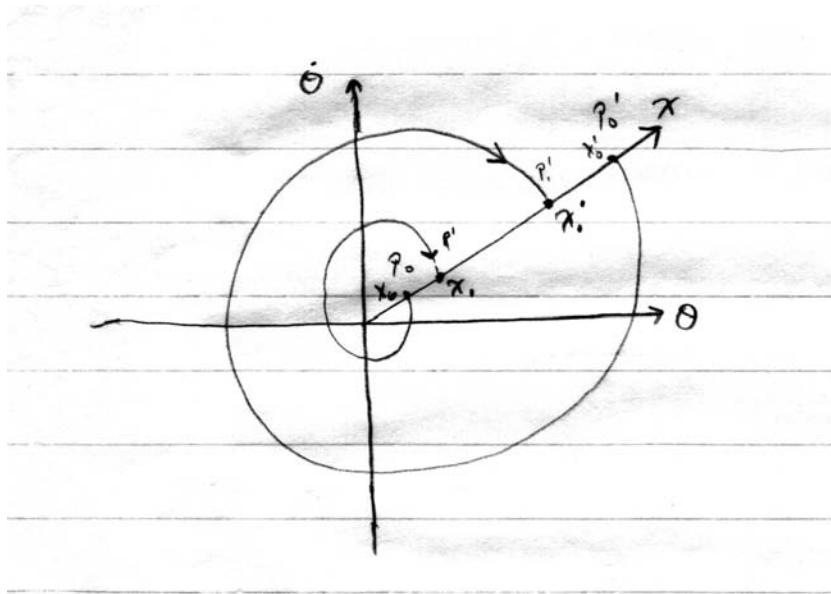
### 8.5.1 Example 1: the van der Pol equation

Consider again the van der Pol equation

$$\frac{d^2\theta}{dt^2} + \varepsilon(\theta^2 - 1)\frac{d\theta}{dt} + \theta = 0$$

Recall that for  $\varepsilon > 0$  the rest position is unstable and that the system has a limit cycle.

We draw a ray emanating from the origin, and consider two representative trajectories initiating and terminating on it:



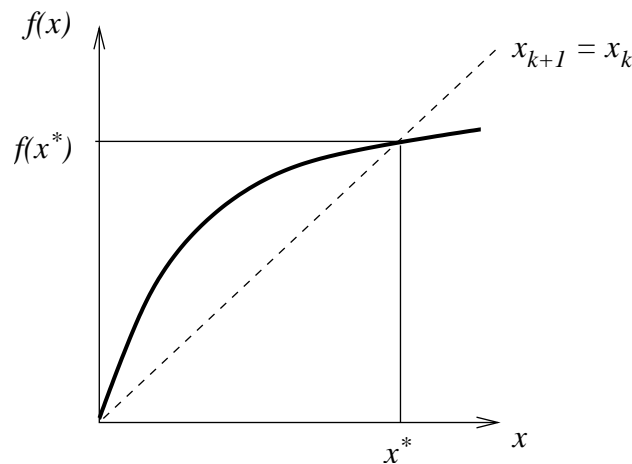
Let  $x_k$  be the position of the  $k$ th intersection of the trajectory with the ray. There is then some mapping  $f$  such that

$$x_{k+1} = f(x_k).$$

The precise form of  $f(x)$  is unknown, but physical and mathematical reasoning allows us to state some of its properties:

- $f$  maps  $x_k$  to a unique  $x_{k+1}$ .
- $f$  is continuous.
- $f'(x) > 1$  near the origin (divergent spirals).
- $f'(x) < 1$  far from the origin (convergent spirals).
- $f'(x) > 0$  for all  $x > 0$  (since  $f(x + \delta) > f(x)$ ).

The simplest form of  $f$  is therefore a curve rising steeply from the origin, followed by a gentle upward slope:



By continuity, there must be a stable fixed point  $x^*$  characterized by

$$x^* = f(x^*) \quad \text{and} \quad f'(x^*) < 1.$$

Thus  $x^*$  gives the effective radius of the stable limit cycle.

### 8.5.2 Example 2: Rössler attractor

Consider the following 3-D flow (the Rössler attractor):

$$\begin{aligned} \dot{x} &= -y - z \\ \dot{y} &= x + ay \\ \dot{z} &= b + z(x - c) \end{aligned}$$

$a$ ,  $b$ , and  $c$  are fixed parameters.

Numerical solutions yield the time series  $x(t)$ :

Figure IV.11, BPV

The time series  $z(t)$ :

Figure IV.11, BPV

A Poincaré section in the  $x$ - $y$  plane:

Figure IV.12a, BPV

And a 3-D perspective of the flow:

Figure 12.1, unknown source

The time series display great irregularity, but the Poincaré section and the full flow display some order.

Consider now another Poincaré section, in the plane

$$y + z = 0.$$

From the Rössler equations, we identify this plane with extrema in the time series  $x(t)$ , i.e., each intersection of the plane corresponds to

$$\dot{x} = 0.$$

Consider a sequence  $x_k$  of such extrema, but only when the extremum is a maximum (local peak) of  $x(t)$ .

Then plot  $x_{k+1}$  vs.  $x_k$ :

Figure IV.10, BPV

Conclusions:

- The 1-D map, even more so than the Poincaré section, reveals that the flow contains much order.
- The time series, however, displays no apparent regularity.

This is the essence of deterministic chaos.

We proceed to show how such Poincaré sections and 1-D maps can be constructed from experimental data.

### 8.5.3 Example 3: Reconstruction of phase space from experimental data

Suppose we measure some signal  $x(t)$  (e.g., the weather, the stock market, etc.)

In most cases it is unlikely that we can specify the equations of motion of the dynamical system that is generating  $x(t)$ .

How, then, may we visualize the system's phase space and its attractor?

The (heuristic but highly successful) idea, originally due to Santa Cruz undergraduates Packer, Crutchfield, Farmer, and Shaw (1980), is to measure any 3 *independent* quantities from  $x(t)$ .

For example:

- $x(t), x(t + \tau), x(t + 2\tau)$ ;  $\tau$  large enough for “independence,” i.e., beyond an autocorrelation time. This is the most popular; it is known as the **method of delays**.
- $x(t), \dot{x}(t), \ddot{x}(t)$  (where the derivatives are finite differences  $x_k - x_{k-1}$ , etc.).

Such a representation of the attractor is not identical to the “real” phase space, but it should retain similar geometric properties.

We use the Rössler attractor as an example.

- Comparison of the projection of the trajectories in the  $x$ - $y$  plane to the projection of the trajectories in the  $x$ - $\dot{x}$  plane:

Figure IV.12, BPV

- Example of different values for  $\tau$  using the method of delays:

Figure 78, Schuster

With the method of delays,  $\tau$  is typically the period of the forcing, or the period of a characteristic limit cycle.

Here we have discussed only qualitative, geometric properties. We shall see that the various representations also yield similar quantitative properties (e.g., measures of Lyapunov exponents).